

General Road Detection Algorithm

A Computational Improvement

Bruno Ricaud, Bogdan Stanculescu and Amaury Breheret

Centre de Robotique, Mines ParisTech, 60 Boulevard St Michel, 75006 Paris, France

Keywords: Vanishing Point, Gabor, Image Processing, Offroad, Computation, Autonomous Driving.

Abstract: This article proposes a method improving Kong et al. algorithm called Locally Adaptive Soft-Voting (LASV) algorithm described in "General road detection from a single image". This algorithm aims to detect and segment road in structured and unstructured environments. Evaluation of our method over different images datasets shows that it is speeded up by up to 32 times and precision is improved by up to 28% compared to the original method. This enables our method to come closer the real time requirements.

1 INTRODUCTION

This work focuses on road detection and reconstruction in semi-natural environment, such as dirt roads, natural pathways or country roads which are hard to follow. Our aim is in providing the driver with a helpful assistance and quantify the difficult conditions that an unprepared road brings. Subsequently, in the future, we plan to apply this kind of assistance to autonomous robots navigation. To this aim, we plan to use monocular ground shape detection, using the watersheds algorithm (Vincent and Soille, 1991; Marcotegui and Beucher, 2005).

In road detection applications the vanishing point plays a central role, for various reasons but mainly for the size reduction of the search area. This reduction usually provides faster computation and better perfor-

mance with less false positives. To create a complete algorithm for road detection we started with vanishing point detection. Kong et al. algorithm is very effective on non-urban roads. One big challenge with this algorithm resides in its computational time which is very long. This is why we have improved its performances and tested the resulting method. Indeed in our application we plan to use real time camera. In this paper, an important part of our contribution is to speed it up to meet the real-time requirements. Thus, our method consists of essentially three contributions over the original algorithm. First we have changed the image transformation, second we have highly increased the computation speed, and finally we have improved the original algorithm precision.

2 VANISHING POINT

2.1 Generalities

When surveying the state of the art, we wanted to test algorithms for vanishing point detection. A road, curved or straight, in urban or non-urban environment, can be modelled as two straight lines which converge on the horizon line. The convergence point is the vanishing point. This point answers three main interrogations : Where is the ground? Where is the sky? Where the road goes?

Different articles (Tardif, 2009; Nieto and Salgado, 2011) and algorithms exists, this problematic is known for few years (Rother, 2002) but Kong's



Figure 1: Vanishing point detection in all type of environment, although without any lane marking.

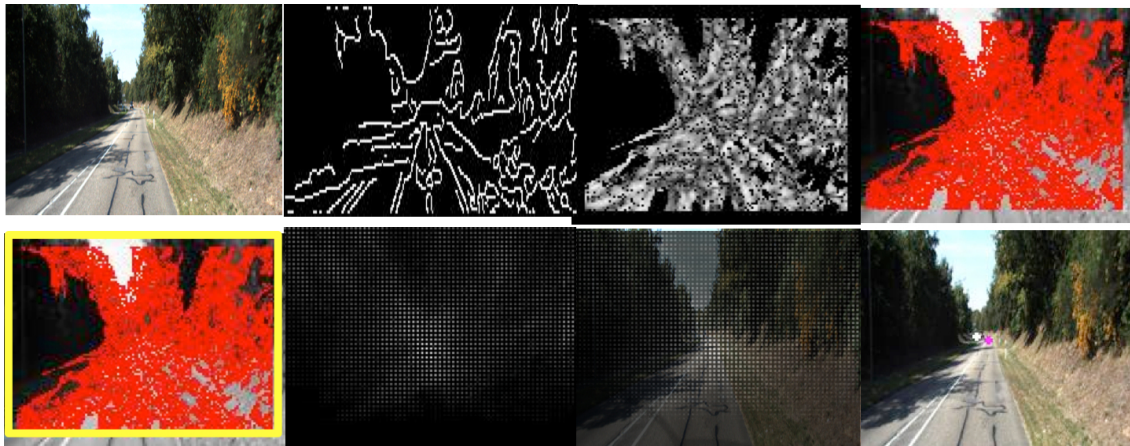


Figure 2: Vanishing Point Detection.

Top row: (1) Starting image. (2) Creation of the edge image. (3) Finding of textures orientations image with Gabor filter. (4) Thresholding of textures orientations map and creation of the confidence map. Bottom row: (5) Candidate pixels vote. (6) Creation of the vote map (7) Election of the most popular pixel of the vote map (8) The vanishing point has been found [PINK], it will be compared to the groundtruth [WHITE].

Locally Adaptive Soft-Voting (LASV) algorithm is the most effective in the spectrum of our application. Indeed LASV is designed to detect roads and pathways in every type of environment(Fig.1) using Gabor filter(Dunn et al., 1995) whereas other methods usually use Hough filter(Maitre, 1985) to detect lanes marking or road borders and are limited to urban situation. In Kong et al. article an entire road segmentation is proposed. For our work we aimed only for vanishing point detection which provides us with all needed information.

2.2 LASV

To summarize LASV we have extracted two step by step tables from (Kong et al., 2010) and we have rewritten them in the following I. and II. table sections. For our method we focus only on the first part of the algorithm which handles vanishing point detection (I. Locally adaptive soft-voting (LASV) scheme).

I. Locally adaptive soft-voting (LASV) scheme (Fig.2)

- 1) For each pixel of the input image, compute the confidence in its texture orientation estimation(computed with the Gabor Filter).(Fig.2.3)
- 2) Normalize the confidence to the range of 0 to 1, and only keep as voters the pixels whose confidence is larger than 0.3(which has been found empirically).(Fig.2.4)
- 3) Only the pixels in the top 90% portion of the image are selected as vanishing point candidates.

4) Create a local voting region R_v , for each vanishing point candidate and only the voters within R_v vote for it.

5) Vote for each vanishing point candidate (Fig.2.6) based on :

$$Vote(P,V) = \begin{cases} \frac{1}{1+(\gamma d(P,V))^2} & , \text{ if } \gamma \geq \frac{5}{1+2d(P,V)} \\ 0 & , \gamma \text{ even} \end{cases} \quad (1)$$

6) The pixel which receives the largest voting score is selected as the initial vanishing point.

II. Vanishing point constrained road border detection

1) Starting from the initially estimated vanishing point vp_0 , construct a set of evenly distributed imaginary rays.

2) For each ray, compute two measures, i.e., OCR^1 and color difference.

3) Select the ray as the first road border if it satisfies the following two conditions:

3.a) It maximizes the following criterion, i.e., :

$$b = arg_i max \left(diff(A1,A2) \times \sum_{j=i-1}^{i+1} OCR_j \right) \quad (2)$$

3.b) Its length is bigger than $\frac{1}{3}$ of the image height.

¹Orientation Consistency Ratio : 1 is a line constituted by a set of oriented points. For each point, if the angle between point orientation and direction line is less than a threshold, the point has a consistent line orientation. OCR is defined as the ratio between the number of consistent points and the number of line points.

4) Update the vanishing point estimation:

4.a) Regularly sample some points (with a four-pixel step) on the first road border denoted p_s .

4.b) Through each point of p_s , respectively construct a set of 29 evenly distributed rays (spaced by 5° , whose orientation from the horizon is more than 20° , and less than 180°) for each point of p_s , denoted as L_s .

4.c) From each L_s , find a subset of n rays such that their OCRs rank top n among the 29 rays.

4.d) The new vanishing point vp_1 is selected from p_s as the one which maximizes the sum of the top n OCRs¹.

5) Starting from vp_1 , detect the second road border in a similar way as the first border, with a constraint that the angle between the road borders is larger than 20° .

3 OUR APPROACH

Our interest in LASV (Kong et al., 2010) is motivated by the possibility of using it as a pre-segmentation for our application. Our implementation aims to work on a vehicle platform equipped with a 30 FPS camera. This is why we needed to accelerate its computation to meet the real time requirements.

We tested this algorithm on several datasets (Geiger et al., 2012; Kong et al., 2010; Leskovec et al., 2008), in our case this algorithm will be used with continuous capture. This is why we have tried to improve this method on datasets using successive frames instead of random environment pictures datasets like the ones used by Kong.

The original code was written in MATLAB by Kong. During the initial tests, the original implementation required a computation time of 18 seconds per image. Our optimisation is mainly concentrated on step I.3) of the original algorithm. Our improvements were done in the same environment in several steps. We have benchmarked each evolution to justify its purpose.

3.1 Methods

For all methods, we have reduced image size down to 240 pixels height and 180 pixels width, just like the original algorithm does. The (Fig.3) illustrates subsequent methods (it shows an asphalt road, indeed this algorithm worked on unmarked and marked

road).

Method I Temporal Dependence

a) For first image, computation of vanishing point research is done on the complete image.

b) For subsequent images, the best vanishing point candidate is only selected from a 10% by 10% image size zone around the coordinates of the vanishing point found previously.

The 10% by 10% range is explained by the fact that the image will not move much between two frames, considering camera preset of 30 FPS. The length of 10% image size has been found empirically.

Method II Reset

a) The temporal method is used but at every 10 frames we do a complete image computation.

Method III Size Reduction

a) Image size is decreased by half before doing the complete image computation. This operation is repeated on every images.

Method IV Temporal + Size Reduction + Reset

a) Image size is decreased by half before computing the vanishing point research.

b) For first image, computation of vanishing point research is done on the complete image.

c) For subsequent images, the best vanishing point candidate is only selected from a 10% by 10% image size zone around the coordinates of the vanishing point previously found in order to refine the vanishing point position.

d) Every 10 images, the computation is done on the complete image.

Method V Downsampling

a) Image size is decreased by half before computing the vanishing point research.

b) Image size is then increased and the best vanishing point candidate is only selected from a 10% by 10% image size zone around the coordinates of the vanishing point found previously on the same but smaller image in order to refine the vanishing point position.

c) These operations are done on every image.

Method VI Temporal + Downsampling + Reset

a) Image size is decreased by half before computing the vanishing point research.

b) Image size is then increased and the best vanishing point candidate is only selected from a 10% by 10% image size zone around the coordinates of the vanishing point previously found on the same but smaller image in order to refine the vanishing point position.

c) The following image size is decreased by a ratio

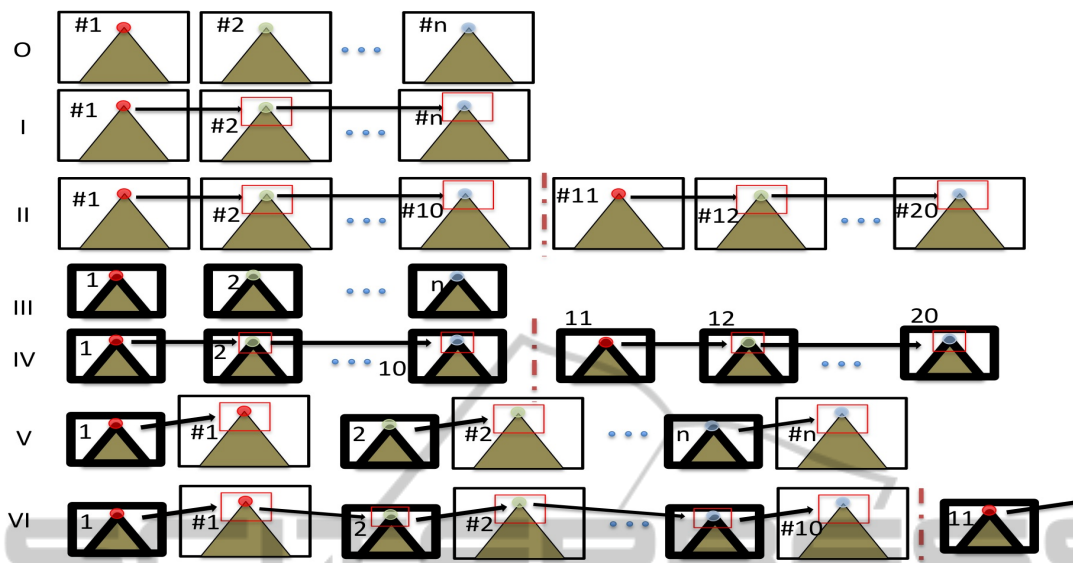


Figure 3: Methods schematic.

O, Original Method : Complete image computation; I, Method I : Arrows show temporal dependency; II, Method II : Dashed bar shows the reset every ten images; III, Method III : Smaller image show image size reduction; ...

before computing the vanishing point only on a 10% by 10% image size zone around the coordinates of the vanishing point found in step b).

d) Image size is then increased and the computation is done only on a 10% by 10% image size zone around the coordinates of the vanishing point previously found in order to refine the vanishing point position.

e) Every 10 images, the computation is done on the complete reduced image.

We also wanted to see the differences in performance between gradient images and edge images. We have compared methods using pre-processed Prewitt images with same methods using in turn pre-processed Canny images.

In order to evaluate the methods we have manually labelled a dataset with the ground-truth location of vanishing points. We used raw data from the Kitti Road dataset (Geiger et al., 2012).

We used two datasets for benchmarking, one also used by LASV author was already labelled with vanishing points, the second has been labelled by our own. All images were used with the resolution 180x240 following author's strategy.

The LASV dataset is composed of 1003 independent images and taken in different environments. This dataset is difficult for algorithm but useful because most of these pictures are missing lane marking and asphalt which make path harder to detect. We used this dataset only on original method and method V. Indeed all temporal method aren't able to be used on

independent images datasets.

The second dataset is a 250 images dataset which are following each other. Ground truth has been labelled using different students estimation. After explaining the vanishing point theory, each student has labelled vanishing points in the datasets. Following these labelling period, we have taken every labelled dataset to compute the average coordinates of vanishing points in each image. This average coordinates are considered as ground truth.

The computation of the local error consists of computing the Euclidean distance between location of the computed vanishing point and its ground-truth location. Global error of each method is the average of all local errors.

This comparison allowed us to created 3 classifications : precision classification, speed classification and speed + precision classification.

3.2 Results

Benchmarking shows a gradual improvement in methods result (Tab.3). From original method to method I we wanted to speed-up the computation by adding a temporal dependency. The temporal dependency provided a small speed-up (Tab.1) but also a big loss in precision (Tab.2). A precision of 65.2% on an image of 180x240 is extremely low, with temporal dependency, vanishing point detection is often lost. This explains method II which was created to decrease the temporal dependency errors. We changed

Table 1: Speed Classification.

Method	Speed (FPS)
Method IV (gradient)	1.96
Method IV (edge)	1.66
Method VI (gradient)	0.71
Method VI (edge)	0.66
Method III (gradient)	0.53
Method I	0.42
Method V (gradient)	0.367
Method III (edge)	0.366
Method V (edge)	0.27
Method II	0.21
Original	0.06

Table 3: Speed * Precision Classification.

Method	#
Method IV (gradient)	1,786
Method IV (edge)	1.41
Method VI (gradient)	0.591
Method VI (edge)	0.526
Method III (gradient)	0,491
Method V (gradient)	0,348
Method III (edge)	0,33
Method V (edge)	0,244
Method II	0,164
Method I	0,143
Original	0,05

Table 2: Precision Classification. Error is the average Euclidian distance between groundtruth and found vanishing point on all the dataset. Precision is this error compared to half the image size.

Method	Precision
Method V (gradient)	94.92%
Original	93.50%
Method III (gradient)	92.66%
Method IV (gradient)	91.12%
Method V (edge)	90.28%
Method III (edge)	90.22%
Method IV (edge)	84.80%
Method VI (gradient)	83.26%
Method VI (edge)	79.74%
Method II	78.06%
Method I	30.41%

Table 4: Precision Classification on ENS Dataset (1003 images in difficult situations). Error is the average Euclidian distance between groundtruth and found vanishing point on all the dataset.

Method	Precision
Original	88.46%
Method V (gradient)	88.01%

dependency to be used only on intervals (10 images). Indeed this method shows us that smaller steps give smaller errors (Tab.2) but a longer computation time (Tab.1). The method III followed the original method where images size is yet decreased. We wanted to see to which point, images size reduction would even bring enough information to be useful. This method revealed to be very effective in both speed and precision (Tab.3).

In method IV we used image reduction and temporal dependency together which shows us very interesting results. Speed had been improved a lot but, a light loss was also present. This is why we have continued to search method which can bring speed-up and precision maintenance. In method V, we used the downsampling method, inspired by the FPDW method (Dollar et al., 2010). We created this method thinking that dependency between two sizes of a same image could bring us more precision (Tab.2) without wasting too much time (Tab.1). This has been confirmed with benchmarks (Tab.3). Method VI was included to show that temporal dependency continues to provide a speed-up but also loses precision (Tab.2)

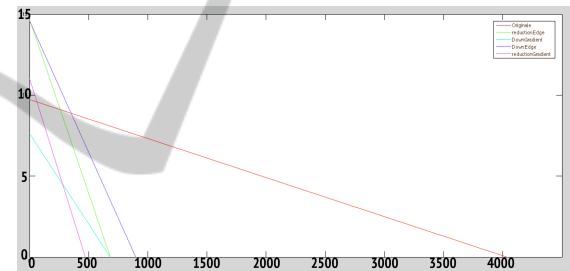


Figure 4: Global Error/ Computation time on 250 images: (red) Original (purple) Method III [gradient] (cyan) Method V [gradient] (green) Method III [edge] (blue) Method V [edge].

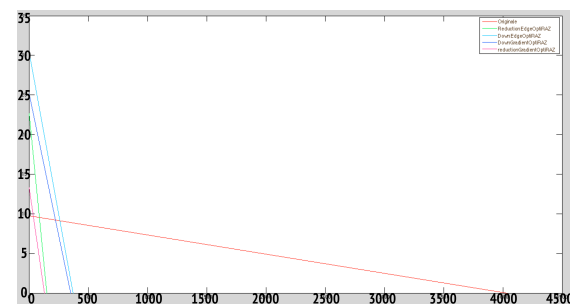


Figure 5: Global Error/ Computation time on 250 images: (red) Original (Pink) Method IV [gradient] (dark blue) Method VI [gradient] (green) Method IV [edge] (clear blue) Method VI [edge].

worse than method II, which shows that too much dependency decreases precision.

Results show that new methods bring speed improvements (fig.5) and precision improvements

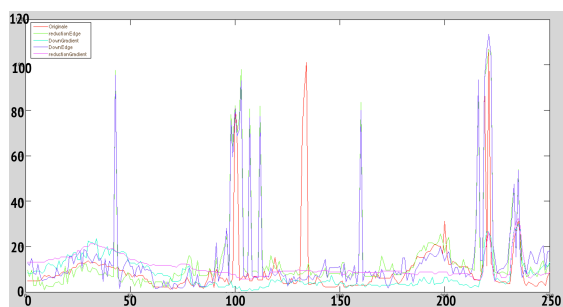


Figure 6: Local errors on each image: (red) Original (purple) Method III [gradient] (cyan) Method V [gradient] (green) Method III [edge] (blue) Method V [edge].

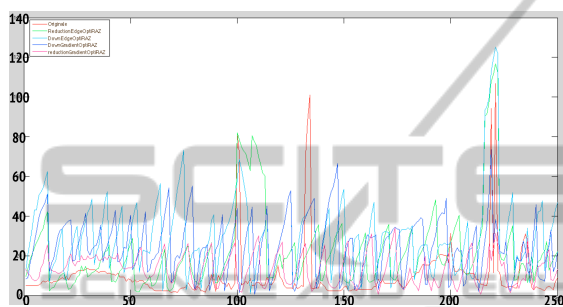


Figure 7: Local errors on each image: (red) Original (pink) Method IV [gradient] (dark blue) Method VI [gradient] (green) Method IV [edge] (clear blue) Method VI [edge].

(fig.4). Results also show that gradient images based methods are faster and more accurate due to the additional information brought by gradient images compared to edge images based methods. The method which is the most efficient is Method IV (Temporal + Size Reduction + Reset). This method does not bring the best precision but is the fastest and is not quite far from original version concerning precision.

4 CONCLUSIONS AND FUTURE WORKS

The obtained results show the entire potential that our improved version of the LASV could have for the pre-segmentation stage. We have improved its precision and speed it up by more than 32 times to come closer to the real time requirements (30 FPS), indeed our improvements are around 2FPS on Matlab compared to the 0.06 FPS of the original LASV. Moreover, our method is almost as precise as the original algorithm. We now plan to create an embedded version of this code and expect to see an additional speed-up compared to the MATLAB implementation. The results would be highly increased and even closer to real time requirements.

We plan to use this pre-segmentation as an aid

for road segmentation using watersheds (Vincent and Soille, 1991; Marcotegui and Beucher, 2005) employing this method to limit the region of interest area and reduce computation time.

REFERENCES

Dollar, P., Belongie, S., and Perona, P. (2010). The Fastest Pedestrian Detector in the West. *Proceedings of the British Machine Vision Conference 2010*, pages 68.1–68.11.

Dunn, D., Higgins, W. E., and Member, S. (1995). Optimal Gabor Filters for Texture Segmentation. 4(7).

Geiger, A., Lenz, P., and Urtasun, R. (2012). Are we ready for autonomous driving? the kitti vision benchmark suite. In *Conference on Computer Vision and Pattern Recognition (CVPR)*.

Kong, H., Audibert, J.-Y., and Ponce, J. (2010). General road detection from a single image. *IEEE transactions on image processing : a publication of the IEEE Signal Processing Society*, 19(8):2211–20.

Leskovec, J., Lang, K. J., Dasgupta, A., and Mahoney, M. W. (2008). Community structure in large networks: Natural cluster sizes and the absence of large well-defined clusters. *CoRR*, abs/0810.1355.

Maitre, L. (1985). Un panorama de la transformation de Hough. 2:305–317.

Marcotegui, B. and Beucher, S. (2005). FAST IMPLEMENTATION OF WATERFALL BASED ON GRAPHS.

Nieto, M. and Salgado, L. (2011). Simultaneous estimation of vanishing points and their converging lines using the {EM} algorithm. *Pattern Recognition Letters*, 32(14):1691 – 1700.

Rother, C. (2002). A new Approach to Vanishing Point Detection in Architectural Environments. (January 2002):1–17.

Tardif, J.-P. (2009). Non-iterative approach for fast and accurate vanishing point detection. *2009 IEEE 12th International Conference on Computer Vision*, (Iccv):1250–1257.

Vincent, L. and Soille, P. (1991). Watersheds in Digital Spaces : An Efficient Algorithm Based on Immersion Simulations. *IEEE transactions on pattern analysis and ...*